

## Synthesis and Improved Acetone Sensing Properties of Porous $\alpha$ -Fe<sub>2</sub>O<sub>3</sub> Nanowires

This article has been downloaded from IOPscience. Please scroll down to see the full text article.

2013 Chinese Phys. Lett. 30 020701

(<http://iopscience.iop.org/0256-307X/30/2/020701>)

View [the table of contents for this issue](#), or go to the [journal homepage](#) for more

Download details:

IP Address: 115.27.96.214

The article was downloaded on 30/08/2013 at 02:44

Please note that [terms and conditions apply](#).

## Synthesis and Improved Acetone Sensing Properties of Porous $\alpha$ -Fe<sub>2</sub>O<sub>3</sub> Nanowires \*

LIU Li(刘丽)<sup>1\*\*</sup>, CHI Xiao(迟霄)<sup>1</sup>, WANG Guo-Guang(王国光)<sup>1</sup>, LIU Chang-Bai(刘唱白)<sup>2</sup>, SHAN Hao(陕皓)<sup>1</sup>, ZHANG Xiao-Bo(张晓波)<sup>1</sup>, WANG Lian-Yuan(王连元)<sup>1</sup>, GUAN Hong-Yu(关宏宇)<sup>3</sup>

<sup>1</sup>State Key Laboratory of Superhard Materials, College of Physics, Jilin University, Changchun 130012

<sup>2</sup>College of Electronic Science and Engineering, Jilin University, Changchun 130012

<sup>3</sup>College of Chemistry, Northeast Normal University, Changchun 130026

(Received 2 August 2012)

Porous  $\alpha$ -Fe<sub>2</sub>O<sub>3</sub> nanowires are synthesized by a simple wet chemical method with a precursor of peroxyacetyl nitrate (PAN), and  $\alpha$ -Fe<sub>2</sub>O<sub>3</sub> nanoparticles are also synthesized in the same way except for the addition of PAN. Gas sensors are fabricated by coating the samples on ceramic tubes with Au signal electrodes and Ni-Cr heaters. A sensing investigation reveals that the porous  $\alpha$ -Fe<sub>2</sub>O<sub>3</sub> nanowires have a higher sensitivity compared to  $\alpha$ -Fe<sub>2</sub>O<sub>3</sub> nanoparticles at 260°C. The corresponding sensor response ( $R_a/R_g$ ) is 18.2 at the maximum to 100 ppm acetone, and the response and recovery times are about 8 and 12 s, respectively. The porous and one-dimensional nanostructures of the porous  $\alpha$ -Fe<sub>2</sub>O<sub>3</sub> nanowires benefit for the gas-absorption and electrical-signal-transfer, and thus improve the sensor sensitivity consequentially.

PACS: 07.07.Df, 82.47.Rs

DOI: 10.1088/0256-307X/30/2/020701

Semi-conducting metal oxides possess a broad range of electrical, chemical and physical properties that are often highly sensitive to changes in the chemical environment.<sup>[1]</sup> Thus various metal oxides are employed in chemical sensors with different performances.<sup>[2]</sup> Traditional sensing materials are nanoparticles,<sup>[3,4]</sup> and the common routes for their sensing enhancements are decreasing their diameters or adding doping metals.<sup>[5]</sup> However, these struggles often fail due to the aggregation growth among the un-ordered nanoparticles.<sup>[6]</sup> Recently, interest in one-dimensional (1D) nanostructures has been greatly stimulated since their sensing properties can be improved in this way.<sup>[7–11]</sup> The high surface-to-volume ratio of 1D nanostructures (a higher surface area provides more sites for analyte molecule adsorption) make them much more sensitive than nanoparticles.<sup>[12,13]</sup> Many high performance sensors have been obtained based on 1D nanomaterials. However, the investigation on the combination of 1D and porous nanostructures is quite rare.<sup>[14–17]</sup> As is known, porous structures can improve the adsorption and desorption of the gases on chemical sensors effectively, thus many have been used for enhancing sensing.

It is well known that  $\alpha$ -Fe<sub>2</sub>O<sub>3</sub> is a traditional sensing material with a versatile performance.<sup>[18–20]</sup> By doping appropriate metals, it can detect both reducing (such as ethanol, acetone, CO, CH<sub>4</sub>, and H<sub>2</sub>) and oxidizing gases (such as Cl<sub>2</sub>, O<sub>2</sub> and NO<sub>x</sub>).<sup>[20]</sup> In this Letter, we report a simple method for the synthesis of porous  $\alpha$ -Fe<sub>2</sub>O<sub>3</sub> nanowires by adding perox-

yacetyl nitrate (PAN) in the precursor solution. PAN is widely chosen for the synthesis of porous carbon nanofibers,<sup>[21]</sup> and porous polymer nanofibers,<sup>[22]</sup> as well as many metal oxides such ZnO and TiO<sub>2</sub> with both porous and 1D nanostructures.<sup>[23–26]</sup> We have prepared various  $\alpha$ -Fe<sub>2</sub>O<sub>3</sub> nanostructures by adjusting PAN in the precursor solution. Here we focus on the comparison between the products with and without PAN. The present porous  $\alpha$ -Fe<sub>2</sub>O<sub>3</sub> nanowires have the highest sensing performance among the obtained  $\alpha$ -Fe<sub>2</sub>O<sub>3</sub> nanostructures. The results provide a simple route to combine the advantages of porous and 1D nanostructures, and thus will be useful for the design of highly sensitive materials.

All chemicals were purchased from Sigma-Aldrich, USA. All chemicals were high purity grades. To synthesize porous  $\alpha$ -Fe<sub>2</sub>O<sub>3</sub> nanowires, 9.0 g of peroxyacetyl nitrate (PAN,  $M_w = 150000$ , 1.184 g/mL at 25°C) was slowly dissolved in 50 mL of *N,N*-dimethylformamide (DMF) at 50°C with vigorous stirring for about 12 h, and then 5 g of FeCl<sub>3</sub>·6H<sub>2</sub>O was added under stirring for another 12 h. Thus, a clear viscous sol solution of PAN/FeCl<sub>3</sub> was obtained by stirring for 5 h in a water bath at 50°C. The solution was added drop-wise into deionized water, and the obtained materials were dried initially for 2 h at 80°C, and then calcined at 600°C for 6 h at a rate of 120°C/h to form porous  $\alpha$ -Fe<sub>2</sub>O<sub>3</sub> nanowires. In this study,  $\alpha$ -Fe<sub>2</sub>O<sub>3</sub> nanoparticles were also prepared in the same way except for the addition of PAN.

X-ray diffraction (XRD) analysis was conducted

\*Supported by the Jilin Environment Office (No 2009-22), Jilin Provincial Science and Technology Department (No 20100344), and the National Innovation Experiment Program for University Students (No 2010C65188).

\*\*Corresponding author. Email: liul99@jlu.edu.cn

© 2013 Chinese Physical Society and IOP Publishing Ltd

on a Scintag XDS-2000 x-ray diffractometer with Cu  $K\alpha$  radiation ( $\lambda = 1.5418 \text{ \AA}$ ). Scanning electron microscopy (SEM) images were performed on a SHIMADZU SSX-550 (Japan) instrument. Transmission electron microscope (TEM) images were obtained on a HITACHI S-570 microscope with an accelerating voltage of 200 kV. The nitrogen isotherms at 77 K were measured using a Micromeritics ASAP 2020M system. The surface area was evaluated using a Brunauer–Emmett–Teller (BET) method.

Sensor parts and sensing measurement were purchased from Beijing Elite Tech Co. Ltd (Beijing, China). The as-calcined sample was mixed with deionized water (resistivity =  $18.0 \text{ M}\Omega/\text{cm}$ ) in a weight ratio of 100:20 to form a paste. The paste was coated on a ceramic tube on which a pair of gold electrodes were previously printed, and then a Ni-Cr heating wire was inserted into the tube to form a side-heated gas sensor.<sup>[27]</sup> The thickness of the sensing film was measured to be about  $300 \mu\text{m}$ . Gas sensing properties were measured using a static test system.<sup>[28]</sup> Saturated target vapor was injected into a test chamber (20 L in volume) by a micro-injector through a rubber plug. After being fully mixed with air (relative humidity was about 25%), the sensor was put into the test chamber. When the response reached a constant value, the sensor was changed to air for recovering the response. The electrical properties of the sensor were measured by a CGS-8 (Chemical Gas Sensing) intelligent analyse system. The response value  $S$  was designated as  $S = R_a/R_g$ , where  $R_a$  is the sensor resistance in air (base resistance) and  $R_g$  is a mixture of target gas and air. The time taken by the sensor resistance to change from  $R_a$  to  $R_a - 90\% \times (R_a - R_g)$  was defined as the response time when the target gas was introduced to the sensor, and the time taken from  $R_g$  to  $R_g + 90\% \times (R_a - R_g)$  was defined as the recovery time when the ambience was replaced by air. Figure 1 shows the synthesizing process and sensing setup of the samples.

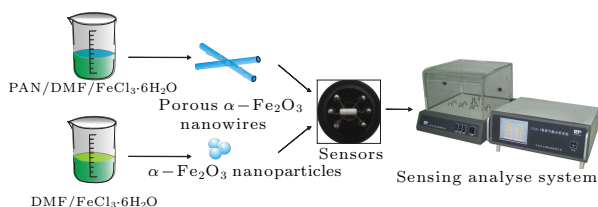
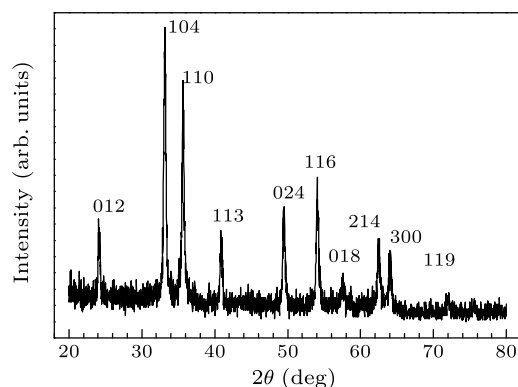


**Fig. 1.** Synthesizing process and sensing setup for porous  $\alpha\text{-Fe}_2\text{O}_3$  nanowires and  $\alpha\text{-Fe}_2\text{O}_3$  nanoparticles.

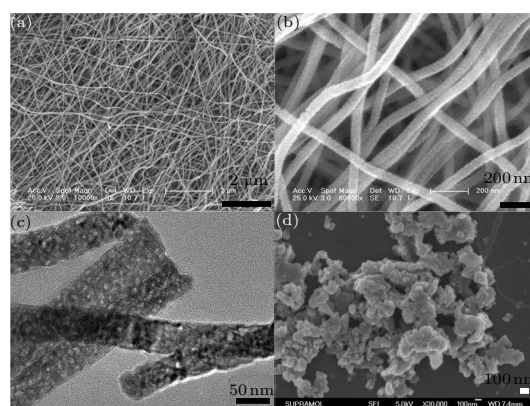
The XRD pattern shown in Fig. 2 indicates the structure of the porous  $\alpha\text{-Fe}_2\text{O}_3$  nanowires. All the peaks in the XRD pattern can be well indexed to hematite (JCPDS:33-0664),<sup>[29]</sup> exposing the formation of the phase-pure spinel  $\alpha\text{-Fe}_2\text{O}_3$ . The pattern of  $\alpha\text{-Fe}_2\text{O}_3$  nanoparticles is similar to that of porous  $\alpha\text{-Fe}_2\text{O}_3$  nanowires in Fig. 2, thus PAN did not change

the crystallization of  $\alpha\text{-Fe}_2\text{O}_3$  evidently.

However, the morphology of  $\alpha\text{-Fe}_2\text{O}_3$  has been evidently affected by PAN. Figures 3(a) and 3(b) show the SEM images of the as-prepared porous  $\alpha\text{-Fe}_2\text{O}_3$  nanowires. The product is highly dominated by the nanowires with lengths of several tens of micrometers and diameters ranging from 30 to 70 nm. The average diameter of the nanowires is about 50 nm. The high-resolution image in Fig. 3(b) clearly reveals that the nanowires are composed of sequential nanoparticles with uniform pores among them. Features of porous  $\alpha\text{-Fe}_2\text{O}_3$  nanowires were also examined by TEM (Fig. 3(c)), which agrees with the SEM results and further confirms the porous structure of the obtained nanowires. Figure 3(d) shows the SEM image of  $\alpha\text{-Fe}_2\text{O}_3$  nanoparticles. Many nanoparticles with an average diameter of about 20 nm are observed.



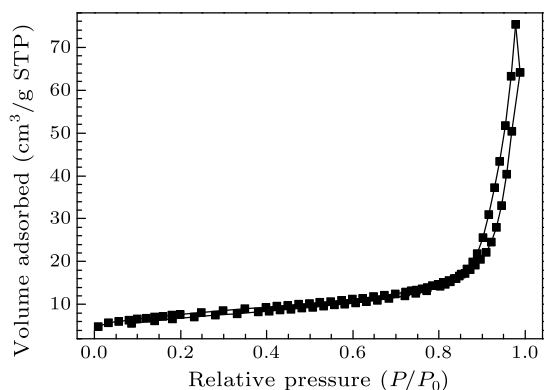
**Fig. 2.** X-ray diffraction pattern of the porous  $\alpha\text{-Fe}_2\text{O}_3$  nanowires.



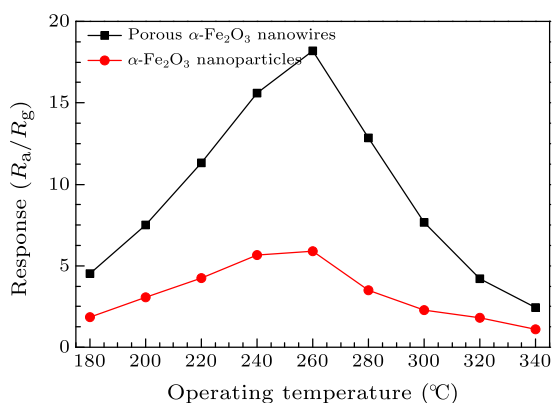
**Fig. 3.** (a) A low-resolution SEM image, (b) a high-resolution SEM image, and (c) TEM image of porous  $\alpha\text{-Fe}_2\text{O}_3$  nanowires; (d) a SEM image of the  $\alpha\text{-Fe}_2\text{O}_3$  nanoparticles.

Figure 4 shows the nitrogen adsorption-desorption isotherms of the porous  $\alpha\text{-Fe}_2\text{O}_3$  nanowires. The isotherms are close to type-II with a strong increase in nitrogen adsorbed volume at a relative pressure higher than 0.85, in which the adsorption and desorption branches of the isotherm almost coincide. Similar isotherms have often been observed in the macropo-

orous materials, indicative of an appreciable amount of macroporosity in the synthesized nanowires.<sup>[30]</sup> This is in agreement with the electron microscopic observation results. The BET surface area is calculated to be  $27.35 \text{ m}^2 \text{ g}^{-1}$ , which is much smaller than many reported  $\alpha\text{-Fe}_2\text{O}_3$  based sensing materials. The explanation for conflict between a low BET surface area and high gas response is shown in the discussion.



**Fig. 4.** Nitrogen adsorption-desorption isotherms of porous  $\alpha\text{-Fe}_2\text{O}_3$  nanowires.



**Fig. 5.** Response values of sensors fabricated from porous  $\alpha\text{-Fe}_2\text{O}_3$  nanowires and  $\alpha\text{-Fe}_2\text{O}_3$  nanoparticles to 100 ppm acetone at different temperatures.

To find out the optimum operating conditions for acetone detection, the sensors fabricated from porous  $\alpha\text{-Fe}_2\text{O}_3$  nanowires and  $\alpha\text{-Fe}_2\text{O}_3$  nanoparticles were exposed to 100 ppm acetone at different temperatures. The response values in Fig. 5 show that both the sensors exhibit their highest response at  $260^\circ\text{C}$ , and this can be explained by considering the same elements forming the samples. The curves exhibit the same tendency, which increases, reaches their maximum, and then decreases with the rising temperature. This characteristic is commonly observed for many semi-conducting metal oxide based sensors, and is based on the influence of the operating temperature on the surface state of the oxygen adsorbates at the steady-state and the activation of oxygen adsorbates of semiconducting metal oxides.<sup>[31,32]</sup> The resis-

tances of the sensors fabricated from porous  $\alpha\text{-Fe}_2\text{O}_3$  nanowires and  $\alpha\text{-Fe}_2\text{O}_3$  nanoparticles at  $260^\circ\text{C}$  in air ( $R_a$ ) are listed in Table 1. The sensors with porous  $\alpha\text{-Fe}_2\text{O}_3$  nanowires show lower resistances, which is due to the fact that the ordered nanostructure of the nanowires can decrease resistance between the nanocrystals, and therefore enhance the film conductance correspondingly.<sup>[5,8,15]</sup>

**Table 1.** Resistances of the sensors fabricated from porous  $\alpha\text{-Fe}_2\text{O}_3$  nanoparticles and  $\alpha\text{-Fe}_2\text{O}_3$  nanowires at different temperatures in air.

Sample	$180^\circ\text{C}$	$220^\circ\text{C}$	$260^\circ\text{C}$	$300^\circ\text{C}$
$\alpha\text{-Fe}_2\text{O}_3$ nanoparticles	111 M $\Omega$	83 M $\Omega$	59 M $\Omega$	24 M $\Omega$
Porous $\alpha\text{-Fe}_2\text{O}_3$ nanowires	22 M $\Omega$	9.3 M $\Omega$	3.8 M $\Omega$	0.9 M $\Omega$

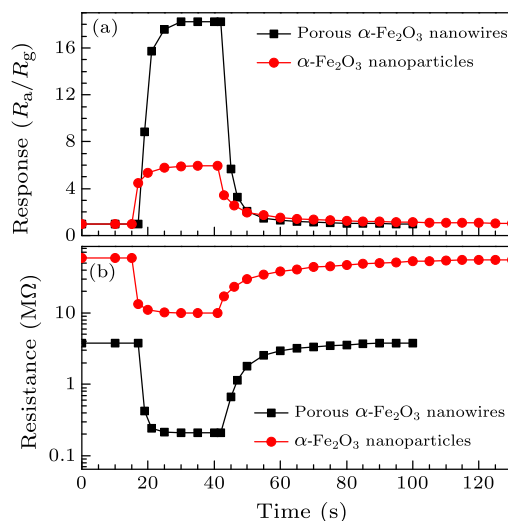


**Fig. 6.** (a) Response-time curves and (b) resistances-time curves of sensors fabricated from porous  $\alpha\text{-Fe}_2\text{O}_3$  nanowires and  $\alpha\text{-Fe}_2\text{O}_3$  nanoparticles to 100 ppm acetone at  $260^\circ\text{C}$ .

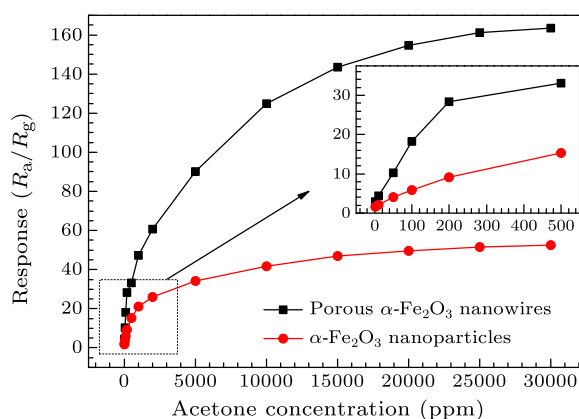


**Fig. 7.** Response values of sensors fabricated from porous  $\alpha\text{-Fe}_2\text{O}_3$  nanowires and  $\alpha\text{-Fe}_2\text{O}_3$  nanoparticles to different concentrations of acetone at  $260^\circ\text{C}$ .

Response and recovery behavior is an important characteristic for evaluating the performance of gas sensors. Figure 6(a) shows the response-recovery curves of sensors fabricated from porous  $\alpha\text{-Fe}_2\text{O}_3$

nanowires and  $\alpha$ -Fe<sub>2</sub>O<sub>3</sub> nanoparticles to 100 ppm acetone at 260°C. The response and recovery times of the sensors based on porous  $\alpha$ -Fe<sub>2</sub>O<sub>3</sub> nanowires are 8 and 12 s, respectively, which are slightly longer than that of the sensors based on  $\alpha$ -Fe<sub>2</sub>O<sub>3</sub> nanoparticles (5 and 10 s). This is because the porous  $\alpha$ -Fe<sub>2</sub>O<sub>3</sub> nanowires have a higher response, which means a large resistance change and longer reaction times of the corresponding sensors (as shown in Fig. 6(b)).

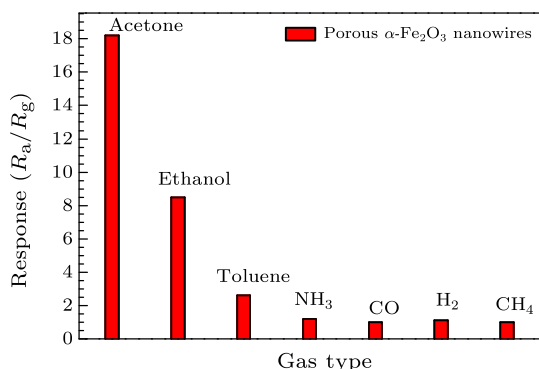


**Fig. 8.** Response values of sensors fabricated from porous  $\alpha$ -Fe<sub>2</sub>O<sub>3</sub> nanowires to 100 ppm different gases at 260°C.

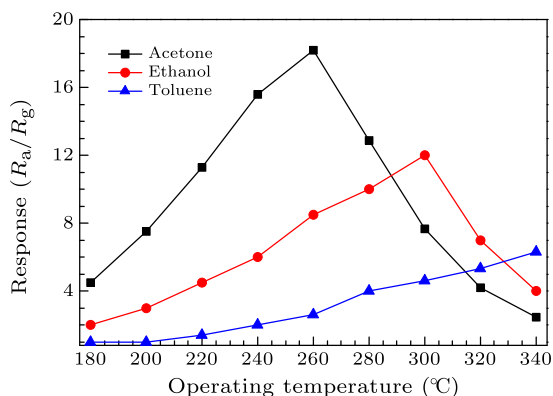


**Fig. 9.** Response values of sensors fabricated from porous  $\alpha$ -Fe<sub>2</sub>O<sub>3</sub> nanowires to 100 ppm acetone, ethanol, and toluene at different temperatures.

Figure 7 shows the sensor response versus acetone concentration at 260°C. The sensors based on porous  $\alpha$ -Fe<sub>2</sub>O<sub>3</sub> nanowires exhibit higher response values in all the tests, proving the improved sensing properties of this material directly. For the porous  $\alpha$ -Fe<sub>2</sub>O<sub>3</sub> nanowire based sensors, their detecting limit is down to 2 ppm (the corresponding response is about 3). Good linearity is found between the response value and acetone concentration in a range from 2 to 200 ppm. The response of the semiconducting oxides can usually be empirically represented as  $R = A \cdot C^N + B$ , where  $A$  and  $B$  are constants, and  $C$  is the concentration of the target gas.  $N$  usually has a value between 0.5 and 1.0, depending on the charge of the surface species and the stoichiometry of the elementary reactions on the sensor surface.<sup>[22,23]</sup> For the

porous  $\alpha$ -Fe<sub>2</sub>O<sub>3</sub> nanowires,  $N$  is around 1 for acetone in the range of 2–200 ppm at 260°C. Such a linear dependence indicates that the obtained nanowires can be used as promising materials for chemical sensors. The saturated concentration of the sensors fabricated from porous  $\alpha$ -Fe<sub>2</sub>O<sub>3</sub> nanowires is about 25000 ppm, which is also much larger than that of the sensors based on  $\alpha$ -Fe<sub>2</sub>O<sub>3</sub> nanoparticles.

The sensor selectivity was tested by exposing the sensors fabricated from porous  $\alpha$ -Fe<sub>2</sub>O<sub>3</sub> nanowires to 100 ppm different gases at 260°C. As shown in Fig. 8, the sensor response to acetone is much higher than that to ethanol, toluene, NH<sub>3</sub>, CO, H<sub>2</sub>, and CH<sub>4</sub>, indicating a good selectivity of the obtained porous  $\alpha$ -Fe<sub>2</sub>O<sub>3</sub> nanowires. The good selectivity is mainly based on the low operating temperature of porous  $\alpha$ -Fe<sub>2</sub>O<sub>3</sub> nanowires to ethanol and other gases. For most semiconducting metal oxides, their optimum temperature is around 300°C.<sup>[6]</sup> The decreased operating condition of 260°C for porous  $\alpha$ -Fe<sub>2</sub>O<sub>3</sub> nanowires to acetone can be attributed to the co-working of the 1D and porous nanostructures of the products.<sup>[5,15,16]</sup> A possible explanation follows.

The base sensing mechanism of  $\alpha$ -Fe<sub>2</sub>O<sub>3</sub> based gas sensors is similar to that of other semiconducting metal oxides such as SnO<sub>2</sub> and ZnO, and the theoretical analysis has been clarified in many previous works.<sup>[33–36]</sup> The most widely accepted model is that the change in resistance of the oxide gas sensors is primarily caused by the adsorption and desorption of the gas molecules on the surface of the sensing film. When  $\alpha$ -Fe<sub>2</sub>O<sub>3</sub> is exposed to air, oxygen adsorbs on the exposed surface of the  $\alpha$ -Fe<sub>2</sub>O<sub>3</sub> and ionizes to O<sup>-</sup> or O<sup>2-</sup> (O<sup>-</sup> is believed to be dominant),<sup>[37]</sup> resulting in a decrease of the carrier concentration and electron mobility. When the  $\alpha$ -Fe<sub>2</sub>O<sub>3</sub> is exposed to a reducing gas (such as acetone in this case), the reducing gas reacts with the adsorbed oxygen molecules and releases the trapped electrons back to the conduction band, thereby increasing the carrier concentration and carrier mobility of  $\alpha$ -Fe<sub>2</sub>O<sub>3</sub>. Thus the resistance change of the  $\alpha$ -Fe<sub>2</sub>O<sub>3</sub> sensors can be found. The reaction between surface oxygen species and acetone can be simply described by



By simply adding PAN to the precursor solution, the original production of  $\alpha$ -Fe<sub>2</sub>O<sub>3</sub> nanoparticles is transformed to porous  $\alpha$ -Fe<sub>2</sub>O<sub>3</sub> nanowires. The acetone sensing properties (especially the response values) have been markedly enhanced. This phenomenon is based on the 1D nanostructure of the as-formed nanowires. The web-like structure can naturally be formed by the 1D nanostructures on the sensor surface, which makes them highly sensitive and efficient transducers of surface chemical processes into electri-

cal signals. Simultaneously, the porous structure of the nanowires is also a key factor for high sensing performance.<sup>[38,39]</sup> Previously, we have prepared the SnO<sub>2</sub> nanofibers with and without porous structures, and the sensing tests show that the nanofibers with some pores on them have a greatly enhanced response. This is because the pores benefit for the sensor to absorb more target gas molecules, and thus improve sensor performance.<sup>[32]</sup> The enhancement of current sensors can also be understood in the same way. However, it should be pointed out that the BET surface area of the porous  $\alpha$ -Fe<sub>2</sub>O<sub>3</sub> nanowires is quite low, because the pores are quite large and non-uniform.<sup>[28,40]</sup>

Although the sensor response value improved greatly, the reacting times only extended slightly. The volcano-type response properties of the obtained sensors can also be explained by considering the 1D structure of the nanowires. The nanowires with large length-to-diameter ratios can transmit electrical signals with high efficiencies.<sup>[12,15]</sup> Simultaneously, the 1D nanostructures can also avoid the aggregation growth among the nanoparticles.<sup>[15]</sup> Compared to 2D nanoscale films, the interfacial areas between the active sensing region of the nanofibers and the underlying substrate are greatly reduced.<sup>[6]</sup> Those advantages lead to significant gain in high response speeds of the as-prepared nanofibers.

Most metal oxides show responses to both reducing and oxidizing gases, and thus often exhibit poor selectivities. The current porous  $\alpha$ -Fe<sub>2</sub>O<sub>3</sub> nanowires have a much higher response to acetone than other gases such as ethanol and toluene. We think that this is because the optimum operating temperature of the nanowires to acetone is much lower than that to other gases. To prove our hypothesis, the sensors were also exposed to 100 ppm ethanol and toluene at different operating temperatures. As can be seen from Fig. 9, the sensor response to acetone decreases with the decreasing operating temperature above 260°C, however the re-

sponse increases in the case of ethanol and toluene. Thus a good selectivity can be obtained under suitable optimum conditions with gases for porous  $\alpha$ -Fe<sub>2</sub>O<sub>3</sub> nanowires.<sup>[8]</sup>

## References

- [1] Janata J et al 1994 *Anal. Chem.* **66** 207
- [2] Neri G et al 2006 *Sens. Actuat. B* **117** 196
- [3] Sahn T et al 2004 *Sens. Actuat. B* **98** 148
- [4] Xu L et al 2011 *Chin. Phys. Lett.* **28** 040701
- [5] Carney C M et al 2005 *Sens. Actuat. B* **108** 29
- [6] Franke M E et al 1994 *Anal. Chem.* **66** 207
- [7] Huang X J et al 2007 *Sens. Actuat. B* **122** 659
- [8] Francioso L et al 2008 *Sens. Actuat. B* **130** 70
- [9] Qiao J P et al 2012 *Chin. Phys. Lett.* **29** 020701
- [10] Kolmakov A et al 2005 *Adv. Mater.* **15** 977
- [11] Kong J et al 2000 *Science* **287** 622
- [12] Liu L et al 2009 *Chin. Phys. Lett.* **26** 090701
- [13] Greiner A et al 2007 *Angew. Chem. Int. Ed.* **46** 5670
- [14] Qi Q et al 2009 *Sens. Actuat. B* **137** 471
- [15] Kolmakov A et al 2004 *Annu. Rev. Mater. Res.* **34** 151
- [16] Pan Z W et al 2001 *Science* **291** 1947
- [17] Jho J H et al 2008 *J. Alloys Comp.* **459** 386
- [18] Yue X J et al 2011 *Chin. Phys. Lett.* **28** 090701
- [19] Moos R et al 2009 *Sensors* **9** 4323
- [20] Ren T Z et al 2004 *Chem. Phys. Lett.* **388** 46
- [21] Par S J et al 2011 *Polym. Int.* **60** 322
- [22] Bayat M et al 2011 *Polymer* **52** 1645
- [23] Qiu Y et al 2009 *Nanoscale. Res. Lett.* **4** 173
- [24] Praharn C et al 2011 *Mater. Lett.* **65** 2498
- [25] Bondarenka V, Grebinskij S, Mickevičius S, Volkov V and Zacharova G 1995 *Sens. Actuat. B* **28** 227
- [26] İnan S et al 2011 *Chem. Eng. J.* **168** 1263
- [27] Qi Q et al 2008 *Sens. Actuat. B* **134** 36
- [28] Zhang Y et al 2008 *Sens. Actuat. B* **132** 67
- [29] Zheng W et al 2009 *Mater. Res. Bull.* **44** 1432
- [30] Ren T Z et al 2004 *Chem. Phys. Lett.* **388** 46
- [31] Pan Z W et al 2001 *Science* **291** 1947
- [32] Qi Q et al 2009 *Sens. Actuat. B* **141** 174
- [33] Liu B et al 2003 *J. Am. Chem. Soc.* **125** 4430
- [34] Ivanovskaya M et al 1998 *Sens. Actuat. B* **53** 44
- [35] Kim S K et al 2010 *Sens. Actuat. B* **149** 28
- [36] Chen Y et al 2009 *Sens. Actuat. B* **137** 291
- [37] Windischmann H et al 1979 *J. Electrochem. Soc.* **126** 627
- [38] Kong J et al 2000 *Science* **287** 622
- [39] Kolmakov A et al 2005 *Nano Lett.* **5** 667
- [40] Yang Z et al 2008 *Sens. Actuat. B* **135** 57